

## THE METALLICITY OF THE REDSHIFT 4.16 QUASAR BR2248-1242\*

CRAIG WARNER<sup>1</sup>, FRED HAMANN<sup>1</sup>, JOSEPH C. SHIELDS<sup>2</sup>, ANCA CONSTANTIN<sup>2</sup>, CRAIG B. FOLTZ<sup>3</sup>,  
& FREDERIC H. CHAFFEE<sup>4</sup>

*Draft version May 21, 2019*

## ABSTRACT

We estimate the metallicity in the broad emission-line region of the redshift  $z = 4.16$  quasar, BR2248-1242, by comparing line ratios involving nitrogen to theoretical predictions. BR2248-1242 has unusually narrow emission lines with large equivalent widths, thus providing a rare opportunity to measure several line-ratio abundance diagnostics. The combined diagnostics indicate a metallicity of  $\sim 2$  times solar. This result suggests that an episode of vigorous star formation occurred near BR2248-1242 prior to the observed  $z = 4.16$  epoch. The time available for this enrichment episode is only  $\sim 1.5$  Gyr at  $z = 4.16$  (for  $H_0 = 65 \text{ km s}^{-1} \text{ Mpc}^{-1}$ ,  $\Omega_m = 0.3$  and  $\Omega_\Lambda \lesssim 1$ ). This evidence for high metallicities and rapid star formation is consistent with the expected early-epoch evolution of dense galactic nuclei.

*Subject headings:* galaxies: active—quasars: emission lines—quasars: individual  
(BR 2248-1242)—galaxies: formation

## 1. INTRODUCTION

The prominent emission line spectra of quasars provide valuable information on the physical state and chemical composition of the gas close to the quasars. If this gas was processed by stars in the surrounding host galaxy then the abundances we measure from the emission lines are a diagnostic of the star formation history in these environments (see Hamann & Ferland 1999 for a general review). At redshifts  $z \gtrsim 4$ , when the universe was only  $\sim 1$  to 2 Gyr old (depending on cosmological models, see Figure 1 in Hamann & Ferland 1999), the results are especially interesting because they provide information about very early star formation, galaxy evolution, and chemical enrichment (Ostriker & Gnedin 1997; Friaca & Terlevich 1998).

Ratios of emission lines involving nitrogen, N, are valuable in determining the metallicity,  $Z$ , because of the expected “secondary” N production via the CNO cycle (Shields 1976). The nitrogen abundance therefore scales as  $Z^2 = (\text{O}/\text{H})^2$  and N/O scales as  $Z = \text{O}/\text{H}$ , providing a sensitive metallicity diagnostic even when direct measures of  $Z = \text{O}/\text{H}$  are not available (Shields 1976; Ferland et al. 1996; Hamann & Ferland 1992, 1993, 1999). Observations of H II regions indicate that secondary nitrogen production dominates for  $Z \gtrsim 0.2 Z_\odot$  (Van Zee et al. 1998; Vila-Costas & Edmunds 1993). When secondary nitrogen production dominates, the N abundance is given by:

$$[\text{N}/\text{O}] \approx [\text{O}/\text{H}] - q \approx \log(Z/Z_\odot) - q \quad (1)$$

where the square brackets indicate logarithmic ratios relative to solar (Hamann et al. 2001). In environments with high star formation rates and short enrichment times, chemical evolution models predict that nitrogen production should be delayed relative to oxygen and carbon. In

Equation 1,  $q$  is the logarithmic offset caused by this delay. It is believed to range from  $\sim 0.0$ – $0.1$  for “slow” chemical evolution, such as in H II regions, to  $\sim 0.2$ – $0.5$  for rapid evolution, such as may occur in massive galactic nuclei (Hamann et al. 2001).

Studies of both emission and absorption lines in quasars suggest that their metallicities are near or above the solar value (Dietrich et al. 1999, 2000; Osmer et al. 1994; Constantin et al. 2001; Petitjean et al. 1994; Hamann 1997; Hamann & Ferland 1999; Hamann et al. 2001). These metallicities are consistent with both observational studies (Pettini 2001) and theoretical simulations (Cen & Ostriker 1999) showing that metal abundances at any time in the universe are dependent on the local density. At every epoch, higher density regions, such as the central regions of galaxies, where quasars reside, should have much higher metallicities than lower density regions such as galactic halos or the intergalactic medium. This dependence of metallicity on density seems to be stronger than any relationship to age (i.e. old does not necessarily mean metal poor). Evidence that density affects metallicity much more than age is found even in our own galaxy, where the central bulge contains many old but metal rich stars (McWilliam & Rich 1994; Idiart et al. 1996).

Much of the previous emission line analysis relied on the line ratios of N V  $\lambda 1240/\text{He II } \lambda 1640$  and N V/C IV  $\lambda 1549$ . Ratios of various weak intercombination lines can be used to test that analysis. In this paper, we measure the emission lines in the rest frame UV spectrum of the high redshift ( $z = 4.16$ ) quasar BR2248-1242, and we examine line ratios involving nitrogen to estimate the metallicity. We selected BR2248-1242 from a sample of 44  $z \gtrsim 4$  quasars in Constantin et al. (2001) because it has unusually narrow emission lines with large equivalent widths, making the

<sup>1</sup>Department of Astronomy, University of Florida, 211 Bryant Space Science Center, Gainesville, FL 32611-2055,  
E-mail: warner@astro.ufl.edu, hamann@astro.ufl.edu Webpage: <http://www.astro.ufl.edu/~warner/BR2248/>

<sup>2</sup>Department of Physics and Astronomy, Ohio University, Athens, OH 45701

<sup>3</sup>MMT Observatory, Tucson, AZ 85721

<sup>4</sup>W. M. Keck Observatory, Kamuela, HI 96743

\*Observations reported here were obtained at the MMT Observatory, a joint facility of the Smithsonian Institution and the University of Arizona.

weak intercombination lines, such as N IV]  $\lambda$ 1486, O III]  $\lambda$ 1664, and N III]  $\lambda$ 1750, easier to detect. This is the most comprehensive emission-line abundance analysis so far for a  $z > 4$  quasar.

## 2. DATA & ANALYSIS

The spectrum of BR2248-1242 was obtained at the MMT Observatory with the Red Spectrograph on September 11, 1994. The full width at half maximum (FWHM) spectral resolution is  $\sim 10$  Å which yields a difference of only  $\sim 10\%$  between the observed and actual FWHM of even the most narrow component. The wavelength range was chosen to span the redshifted Ly $\alpha$   $\lambda$ 1216 to N III]  $\lambda$ 1750 interval. This corresponds to an observed wavelength range of  $\sim 5500$  Å to nearly 10,000 Å. The observation and data reduction details are discussed in Constantin et al. (2001). Figure 1 shows the observed spectrum.

We measured the emission lines using tasks in the IRAF<sup>5</sup> software package. We obtained the Galactic H I column density (Dickey & Lockman 1990) and calculated a reddening of  $E_{B-V} = 0.0693$ . We then performed a reddening correction and used the task NFIT1D to fit the continuum with a powerlaw of the form  $F_\nu \propto \nu^\alpha$ . The fit has a spectral index,  $\alpha = -1.09$  (see Figure 1) and is constrained by the flux in wavelength intervals between the emission lines, namely 6913–6991 Å, 8733–8898 Å, and 9278–9777 Å. We next used the task SPECFIT (Kriss 1994), which employs a  $\chi^2$  minimization routine, to fit each line with one or more Gaussian profiles. Figure 2 shows the fits. Table 1 lists the line fluxes and rest-frame equivalent widths (REWs) as measured above the fitted continuum. The fluxes, REWs, and FWHMs given in Table 1 are from the total fitted profiles, which can include several multiplet components and up to 3 Gaussian profiles per component (see below). Table 2 lists the rest wavelength, flux, REW, and FWHM of each individual Gaussian profile. We calculate the emission line redshift to be  $z = 4.156$  based on the narrow Gaussian profiles fit to Ly $\alpha$  and C IV. We use this redshift to calculate the rest wavelength for each component.

We fit C IV  $\lambda$ 1549 with three Gaussian profiles, including a very broad profile (FWHM  $\approx 22500$  km s $^{-1}$ ). This broad pedestal includes the unidentified  $\sim 1600$  Å emission feature that has been noted in earlier studies (Laor et al. 1994; Boyle 1990; Wilkes 1984). We ignore the doublet splitting in C IV because it is small compared to the observed line widths. N IV]  $\lambda$ 1486, He II  $\lambda$ 1640, and O III]  $\lambda$ 1664 are all fit with one Gaussian profile. Each component of the Si II  $\lambda\lambda$ 1527, 1533 and Si IV  $\lambda\lambda$ 1393, 1403 doublets are fit with one Gaussian profile. The fluxes of these components are tied to a 1:1 ratio because this yields a better fit than a 2:1 ratio. In every multiplet fit, we fix the ratio of the central wavelengths to the known ratio of the rest wavelengths and tie together the FWHMs of each component. The N III]  $\lambda$ 1750 and O IV]  $\lambda$ 1403 multiplets are fit with one Gaussian profile for each of their 5 components. The flux component ratios in these cases are tied to the ratio of the statistical weight  $g$  times the  $A$  value for each transition, using atomic data obtained from the National Institute of Standards and Technol-

ogy (<http://aeldata.phy.nist.gov/PhysRefData/contents-atomic.html>) and Nussbaumer & Storey (1982). Ly $\alpha$   $\lambda$ 1216 is fit with three Gaussian components, with only the red side used for  $\chi^2$  minimization because of contamination by the Ly $\alpha$  forest on the blue side. Each component of the N V  $\lambda$ 1240 doublet is fit with two Gaussian profiles with FWHMs fixed to the values obtained from the narrow and intermediate width profiles of our fit to C IV. This connection between C IV and N V can be justified because they are both high ionization lines with similar excitation and emission properties (Dietrich & Wilhelm-Erkens 2000). The relative fluxes of the two components of the N V doublet are set to 2:1 for each component, again because this yields a better fit than a 1:1 ratio. We fit the Si II  $\lambda\lambda$ 1260, 1264, 1265 triplet with one Gaussian profile for each of the three components. Because the flux of Si II is so much smaller than Ly $\alpha$  and N V, Si II is not well defined by the  $\chi^2$  minimization.

The primary uncertainty in our flux measurements is the continuum location. Many of the lines are blended, which introduces more uncertainty, particularly for N V in the wing of Ly $\alpha$ . The broad component in the C IV fit introduces another uncertainty because it includes the  $\sim 1600$  Å feature. We do not include this broad component in our calculated of flux ratios (§3 below) because it is believed to be an unrelated emission feature (Laor et al. 1994). We estimate the one  $\sigma$  standard deviation of our measurement of the flux of Ly $\alpha$  to be  $\sim 10\%$  based on repeated measurements with the continuum drawn at different levels. By the same method, we estimate the uncertainty in C IV, N V, He II, and O III] to be  $\sim 15$ –20% and the uncertainty in the remaining lines with REW  $\leq 10$  Å to be  $\sim 25\%$ .

## 3. RESULTS

Table 3 lists various measured flux ratios and the metallicities inferred from comparisons to the theoretical results from Hamann et al. (2001). Our preferred estimates of the metallicity are obtained from the model in Hamann et al. that uses a segmented powerlaw for the photoionizing continuum shape (see Figure 3). This continuum shape is a good approximation to the average observed continuum in quasars (Zheng et al. 1997; Laor et al. 1997). The metallicity ranges in Table 3 represent the range of results obtained by comparisons to all three different continuum shapes calculated by Hamann et al. and shown in Figure 3. These theoretical uncertainties are in addition to any uncertainty in the measured line strengths (§2).

All of the line ratios in Table 3 yield a metallicity of  $Z \approx 1$ –3 Z $_{\odot}$ . From a theoretical viewpoint, N III]/O III] is the most reliable of the intercombination line ratios (Hamann et al. 2001). N V/He II is also a useful ratio, whereas N IV]/O III] and N IV]/C IV can be unreliable because they are more sensitive to non-abundance effects and generally yield a wider range of results than N III]/O III]. Based on which ratios are most accurately measured, and which are most reliable from a theoretical viewpoint (Hamann et al. 2001), we estimate the overall metallicity of BR2248-1242 to be roughly  $Z \approx 2$  Z $_{\odot}$ .

It is important to note, however, that the actual metallicity of BR2248-1242 may be 2–3 times higher than  $Z \approx$

<sup>5</sup>The Image Reduction and Analysis Facility (IRAF) is distributed by the National Optical Astronomy Observatories, which is operated by the Association of Universities for Research in Astronomy, Inc. (USRA), under cooperative agreement with the National Science Foundation.

$2 Z_{\odot}$  because the theoretical models we use assume  $q \approx 0$  in Equation 1. For environments with rapid chemical evolution, such as massive galactic nuclei,  $q \approx 0.2\text{--}0.5$  may be more appropriate (Hamann et al. 2001). Therefore, the metallicity of BR2248-1242 is broadly consistent with previous emission line results of  $Z \approx 1\text{--}9 Z_{\odot}$  derived for other quasars (Hamann et al. 2001; Dietrich & Wilhelm-Erkens 2000; Hamann & Ferland 1999; Korista et al. 1998; Ferland et al. 1996).

For any appropriate  $q$  value, BR2248-1242 may still yield a lower bound on the metallicity of luminous quasars because it appears to have an unusually low black hole mass (and so may reside in a lower mass, lower metallicity galaxy). We estimate the black hole mass in BR2248-1242 to be  $M_{BH} \approx 4.77 \times 10^8 M_{\odot}$ , based on the measured FWHM of C IV and the formulae given in Kaspi et al. (2000)

$$R_{\text{BLR}} = (32.9_{-1.9}^{+2.0}) \left[ \frac{\lambda L_{\lambda}(5100\text{\AA})}{10^{44} \text{ ergs s}^{-1}} \right]^{0.700 \pm 0.033} \text{ lt-days} \quad (2)$$

$$M = 1.464 \times 10^5 \left( \frac{R_{\text{BLR}}}{\text{lt-days}} \right) \left( \frac{v_{\text{FWHM}}}{10^3 \text{ km s}^{-1}} \right)^2 M_{\odot} \quad (3)$$

where  $R_{\text{BLR}}$  is the radius of the broad line region for  $H\beta$ , and  $R_{\text{BLR}}(\text{C IV}) \approx 0.5 R_{\text{BLR}}(H\beta)$  is the radius of the C IV region (Peterson 2001). The FWHM of C IV (1620  $\text{km s}^{-1}$ ) is represented by  $v_{\text{FWHM}}$  and  $M$  is the mass of the black hole. We derive  $\lambda L_{\lambda}(1450\text{\AA})$  from the observed flux (Dietrich et al. 2002 in preparation) and use a power-law of the form  $F_{\nu} \propto \nu^{\alpha}$  with  $\alpha = -0.4$  to approximate the continuum shape and estimate  $\lambda L_{\lambda}(5100\text{\AA})$ . We select  $\alpha = -0.4$  based on average quasar spectra from Vanden Berk et al. (2001) and Dietrich et al. (2002 in preparation). The derived black hole mass in BR2248-1242 is unusually low because of its unusually narrow emission lines. Previous studies suggest a correlation between black hole mass and the overall bulge/spheroidal component mass of the surrounding galaxy (Gebhardt et al. 2001; Ferrarese & Meritt 2000; Laor 2001; Wandel 1999). Together with the well known relationship between the mass and metallicity of galaxies (Faber 1973; Zaritsky et al. 1994; Jablonka et al. 1996), these results predict a relationship between the mass of the black hole and the metallicity surrounding the quasar (Warner et al. 2002 in preparation). BR2248-1242 appears to have a low black hole mass, and so may be expected to have relatively low metal abundances.

#### 4. DISCUSSION

The result for  $Z \gtrsim Z_{\odot}$  in BR2248-1242 suggests that an episode of rapid and extensive star formation occurred before the observed  $z = 4.16$  epoch. The spectral similarity of BR2248-1242 to other  $z > 4$  quasars (apart from the narrow line widths, see Constantin et al. 2001) suggests further that the results for  $Z \gtrsim Z_{\odot}$  should apply generally. The time available for the chemical enrichment at  $z = 4.16$  is only  $\sim 1.5$  Gyr (for  $H_0 = 65 \text{ km s}^{-1} \text{ Mpc}^{-1}$ ,  $\Omega_m = 0.3$  and  $\Omega_{\Lambda} \lesssim 1$ ). This star formation episode early in the history of the universe would be consistent with observations showing that the central regions of massive galaxies today contain old, metal rich stars (McWilliam & Rich 1994; Bruzual et al. 1997; Worthey et al. 1992; Idiart et al. 1996). This high redshift evolution would

also be well within the parameters derived in some recent simulations, which show that the densest proto-galactic condensations can form stars and reach solar or higher metallicities at  $z \gtrsim 6$  (Ostriker & Gnedin 1997; Haiman & Loeb, 2001). Recent observations of the highest redshift quasars suggest that reionization occurred around  $z \sim 6$  (Becker et al. 2001; Djorgovski et al. 2001). If the reionization is due to stars, this would provide further evidence for substantial star formation beginning at  $z \gtrsim 6$ . Quasar abundance studies can provide observational tests of these evolution scenarios. The next step is clearly to extend the abundance analysis to the highest possible redshifts, and to compare the results across wide ranges in redshift, host galaxy types, and central black hole mass.

*Acknowledgements:* We are grateful to Matthias Dietrich, Bassem Sabra, Eric McKenzie, and Catherine Garland for their comments on this manuscript. We acknowledge financial support from the NSF via grants AST99-84040 and AST98-03072.

## REFERENCES

Becker, R. H. et al. 2001, AJ, in press

Boyle, B. J. 1990, MNRAS, 243, 231

Bruzual, G., Barbuy, B., Ortolani, S., Bica, E. & Cuisinier, F. 1997, AJ, 114, 1531

Cen, R., Ostriker, J. P. 1999, ApJ, 519, L109

Constantin, A., Shields, J. C., Hamann, F., Foltz, C. & Chaffee, F. 2001, ApJ, in press

Dickey, J. & Lockman, F. 1990, ARA&A, 28, 215

Dietrich, M. et al. 1999, A&A, 352, L1

Dietrich, M. & Wilhelm-Erkens, U. 2000, A&A, 354, 17

Dietrich, M., Hamann, F. et al. 2002, in preparation

Djorgovski, S. G., Mastro, S. M., Stern, D., Mahabal, A. A. 2001, ApJ, in press

Faber, S. M. 1973, ApJ, 179, 423

Ferland, J. et al. 1996, ApJ, 461, 683

Ferrarese, L. & Merritt, D. 2000, ApJ, 539, L9

Friaca, A. C. S. & Terlevich, R. J. 1998, MNRAS, 289, 399

Gebhardt, K., Bender, R., Bower, G., Dressler, A., Faber, S. M., et al. 2000, ApJ, 539, L13

Haiman, Z. & Loeb, A. 2001, ApJ, 552, 459

Hamann, F. & Ferland, G. 1992, ApJ, 391, L53

Hamann, F. & Ferland, G. 1993, ApJ, 418, 11

Hamann, F. 1997, ApJS, 109, 279

Hamann, F. & Ferland, G. 1999, ARA&A, 37, 487

Hamann, F., Korista, K. T., Ferland, G. J., Warner, C., & Baldwin, J. 2001, ApJ, in press

Idiart, T. P., de Freitas Pacheco, J. A. & Costa, R.D.D. 1996, AJ, 112, 2541

Jablonka, P., Martin, P., & Arimoto, N. 1996, AJ, 112, 1415

Kaspi, S., Smith, P. S., Netzer, H., Maoz, D., Jannuzi, B. T., Giveon, U. 2000, ApJ, 533, 631

Korista, K.T. Baldwin, J. & Ferland, G.J. 1998, ApJ, 507, 24

Kriss, G. 1994, in ASP Conf. Ser. 61, Astronomical Data Analysis Software and Systems III, eds. D. R. Crabtree, R. J. Hanisch, & J. Barnes (San Francisco: ASP), 437

Laor, A. et al. 1994, ApJ, 420, 110

Laor, A., Jannuzi, B. T., Green, R. F. & Boroson, T. A. 1997, ApJ, 489, 656

Laor, A. 2001, ApJ, 553, 677

McWilliam, A. & Rich, R. M. 1994, ApJS, 91, 749

Nussbaumer, H. & Storey, P. J. 1982, A&A, 115, 205

Osmer, P., Porter, A. C. & Green, R. F. 1994, ApJ, 436, 678

Ostriker, J. & Gnedin, O. 1997, ApJ, 487, 667

Peterson, B. M. 2001 in Advanced Lectures on the Starburst-AGN Connection, ed. I.Aretxaga, D. Kunth, R. Mújica, World Scientific Publ., p. 3

Petitjean, P., Rauch, M. & Carswell, R. F. 1994, A&A, 291, 29

Pettini, M. 2001 in 'The Promise of FIRST' symposium, 12-15 December, 2000, ed G.L. Pillbratt, J. Cernicharo, A.M. Heras, T. Prusti, & R. Harris. Toledo, Spain.

Shields, G. A. 1976, ApJ, 204, 330

Van Zee, L., Skillman, E. D. & Salzer, J. J. 1998, ApJ, 497, L1

Vanden Berk, D. E. et al. 2001, AJ, 122, 549

Vila-Costas, M. B. & Edmunds, M. G. 1993, MNRAS, 265, 199

Wandel, A. 1999, ApJ, 519, L39

Warner, C., Hamann, F., Dietrich, M., Shields, J. C., Constantin, A., & Junkkarinen, V. 2002, in preparation

Wilkes, B. J. 1984, MNRAS, 207, 73

Worley, G., Faber, S. M. & Gonzalez, J. 1992, ApJ, 398, 69

Zaritsky, D., Kennicutt, R. C., & Huchra, J. P. 1994, ApJ, 440, 606

Zheng, W., Kriss, G. A., Telfer, R. C., Grimes, J. P. & Davidsen, A. F. 1997, ApJ, 475, 469

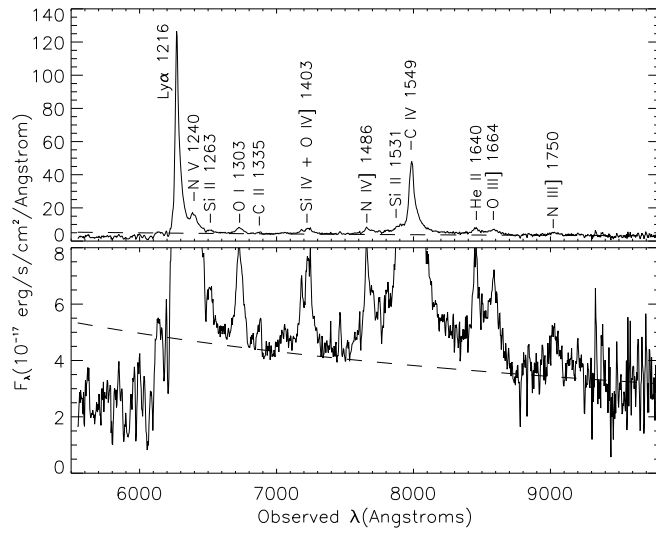


FIG. 1.— Spectrum of BR2248-1242 with our fit to the continuum overplotted (dashed line). The spectrum has been corrected for extinction.

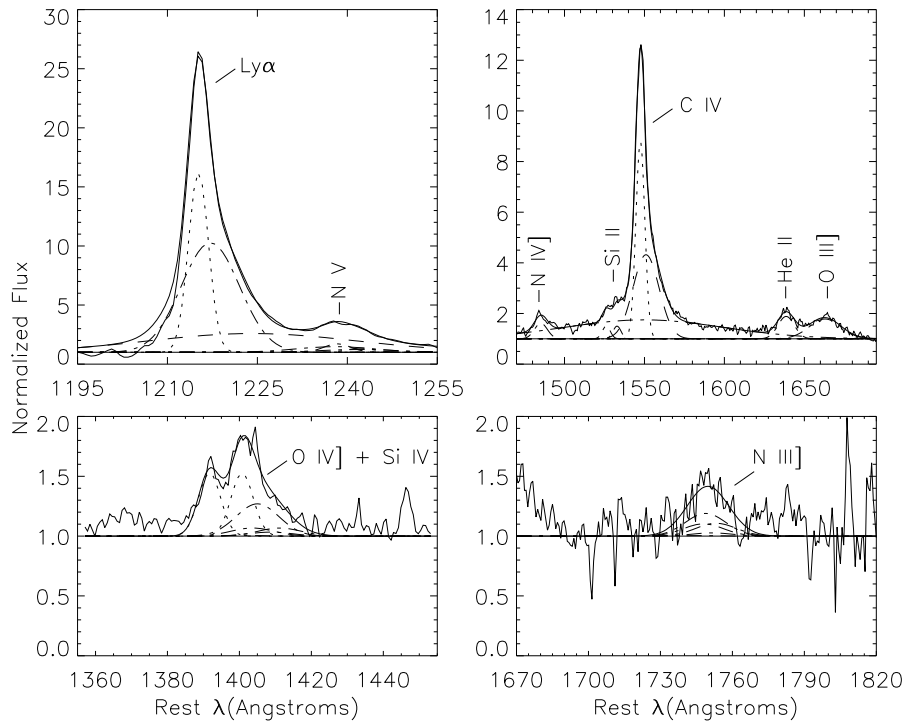


FIG. 2.— Gaussian fits of emission lines of BR2248-1242. The continuum is normalized by the power law fit shown in Figure 1. The continuum (at unity) and composite line fits are plotted as solid curves. The individual components of the fits are shown as dotted and dashed lines. Larger versions of these plots are available at <http://www.astro.ufl.edu/~warner/BR2248/>.

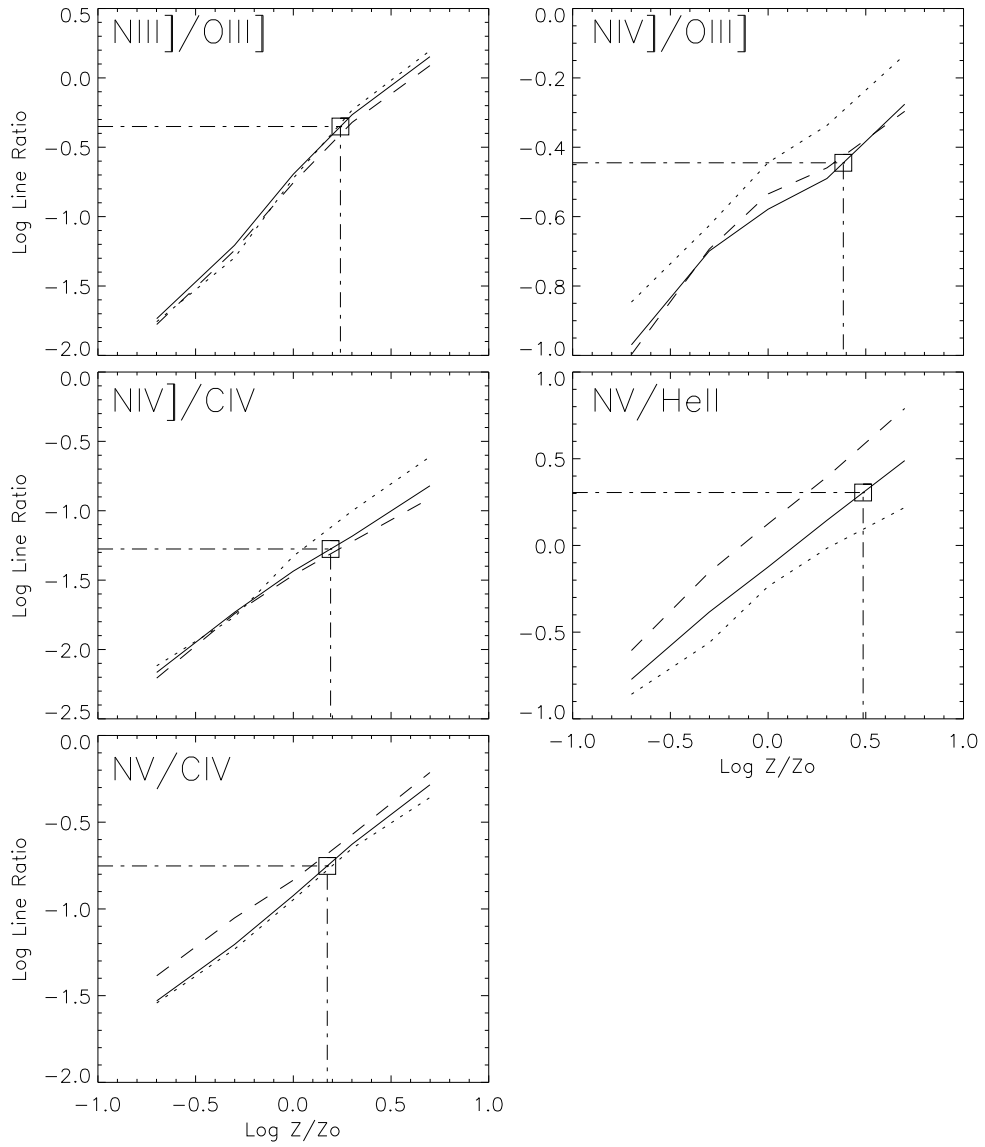


FIG. 3.— Comparison of flux ratios measured in BR2248-1242 to theoretical results from Figure 5 of Hamann et al. (2001). Comparisons of our measured line ratios to the theoretical model represented by the solid line yield our preferred estimates for metallicity. The solid line is obtained from the model in Hamann et al. that uses a segmented powerlaw for the photoionizing continuum shape, which is a good approximation to the average observed continuum in quasars. The dotted line corresponds to the model that uses an incident spectrum defined by Matthews & Ferland (1987), while the dashed line corresponds to a powerlaw with index  $\alpha = -1.0$  across the infrared through X-rays .

TABLE 1  
EMISSION LINE DATA

Line	$\lambda_{obs}^a$	Flux <sup>b</sup>	Flux/Ly $\alpha$	REW <sup>a</sup>	FWHM <sup>c</sup>
Ly $\alpha$ $\lambda$ 1216	6270.3	6040	1.000	246	1450
N V $\lambda$ 1240	6396.6	420	0.070	18	2380
Si II $\lambda$ 1263	6509.9	90	0.014	4	3660
O I $\lambda$ 1303	6728.7	250	0.041	10	3020
C II $\lambda$ 1335	6874.2	30	0.005	1	1270
Si IV $\lambda$ 1397	7204.5	180	0.029	8	3490
O IV] $\lambda$ 1403	7254.8	140	0.023	7	3240
N IV] $\lambda$ 1486	7663.9	130	0.021	6	1910
Si II $\lambda$ 1531	7892.1	120	0.020	6	2450
C IV $\lambda$ 1549	7984.8	2400	0.398	122	1620
He II $\lambda$ 1640	8455.3	210	0.035	11	2200
O III] $\lambda$ 1665	8580.6	350	0.059	19	4200
N III] $\lambda$ 1751	9029.2	160	0.026	9	3530

<sup>a</sup> In units of Å

<sup>b</sup> In units of  $10^{-17}$  ergs cm $^{-2}$  s $^{-1}$

<sup>c</sup> In units of km s $^{-1}$

TABLE 2  
EMISSION LINE COMPONENTS

Component	$\lambda_{rest}^a$	Flux <sup>b</sup>	REW <sup>a</sup>	FWHM <sup>c</sup>
Ly $\alpha$ 1	1216.1	1580	64	970
Ly $\alpha$ 2	1218.1	2780	112	2810
Ly $\alpha$ 3	1225.1	1690	69	10020
N V 1	1240.2	140	6	1280
N V 2	1240.6	280	12	3710
Si II	1262.8	90	4	3390
O I	1305.0	250	10	3020
C II	1333.2	30	1	1230
Si IV	1397.3	180	8	1570
O IV]	1407.1	140	7	3000
N IV]	1486.3	130	6	1910
Si II	1530.7	120	6	1140
C IV 1	1548.6	1070	55	1280
C IV 2	1552.2	1330	68	3710
C IV 3	1551.0	1820	93	22570
He II	1639.9	210	11	2200
O III]	1664.2	350	19	4200
N III]	1751.2	160	9	3390

<sup>a</sup> In units of Å

<sup>b</sup> In units of  $10^{-17}$  ergs cm $^{-2}$  s $^{-1}$

<sup>c</sup> In units of km s $^{-1}$

TABLE 3  
EMISSION LINE RATIOS

Lines	Ratio	Z/Z <sub>⊙</sub>
N III]/[O III]	0.45	$1.74^{+0.16}_{-0.05}$
N IV]/[O III]	0.36	$2.43^{+0.00}_{-1.20}$
N IV]/[C IV]	0.05	$1.55^{+0.16}_{-0.44}$
N V/He II	2.02	$3.07^{+3.94}_{-1.48}$
N V/[C IV]	0.18	$1.49^{+0.09}_{-0.25}$